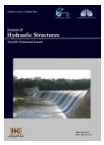
Journal of Hydraulic Structures
***J. Hydraul. Struct.*, 2018; 4(1):19-35**
DOI: 10.22055/JHS.2018.25309.1070



OPEN ACCESS

Wave Evolution in Water Bodies using Turbulent MPS Simulation

Hanifeh Imanian[1]
Morteza Kolahdoozan[2]
Amir Reza Zarrati[3]

Abstract

Moving Particle Semi-implicit (MPS) which is a meshless and full Lagrangian method is employed to simulate nonlinear hydrodynamic behavior in a wide variety of engineering application including free surface water waves. In the present study, a numerical particle-based model is developed by the authors using MPS method to simulate different wave problems in the coastal waters. In this model fluid and solid are treated as separate phases and governing equations of momentum and continuity are solved for them concurrently. For simulations of turbulent wavy flows, constant eddy viscosity, Prandtl's mixing length theory and k-ε models were considered. In addition, higher order of MPS operators was applied to suppress numerical oscillation in comparison with previous studies. The developed method was applied to some cases, including still water reservoir, solitary wave propagation in a tank, tsunami run-up on an inclined wall and wave generation due to the landslide. Evaluation of the developed model results, in compare with data cited in the literature showed enhancement in the accuracy of the developed numerical model especially in compare with existing inviscid models. Besides, the numerical tests results have shown that applying k-ε turbulence model, have equipped MPS model with a useful, powerful and reliable tool for simulating water free surface in wave motion, wave impact and the breaking process.

Keywords: numerical modeling, Lagrangian approach, Moving Particle Semi-implicit (MPS) method, turbulence modeling, wave evolution

Received: 18 March 2018; Accepted: 25 May 2018

[1] Assistant professor, Department of Civil Engineering, Engineering Faculty, Alzahra University, Tehran, Iran, h.imanian@alzahra.ac.ir (**Corresponding author**)
[2] Associate professor, Department of Civil and Environmental Engineering, Amirkabir University of Technology, Tehran, Iran, mklhdzan@aut.ac.ir
[3] Professor, Department of Civil and Environmental Engineering, Amirkabir University of Technology, Tehran, Iran, zarrati@aut.ac.ir

CC BY

1. Introduction

Owing to commercial and economical role in coastal areas, studying waves have significant hydraulic importance especially in marine environments and estuaries. Hydrodynamic simulation of wave mechanics is however difficult due to complexity of their boundary conditions which are incorporated with an arbitrary moving surface. Despite the great advances in numerical modeling, it is still difficult to simulate free surfaces or solid- fluid interactions like wave impact to coastal structures.

Recently, Lagrangian approaches are applied in free surface modeling [1]. According to this approach, the study area is divided into a number of particles and the governing equations of flow are discretized and solved for each particle [2]. In particle-based methods no mesh generation is required and therefore free surface can be predicted by tracking fluid particle positions in each time step. This means no additional equation is necessary to be solved for free surface prediction. Since no mesh is necessary, the numerical dispersion errors, which are related to mesh generation, are eliminated.

The first ideas in this way were proposed by Monaghan in the area of astrophysical hydrodynamic problems with the method called Smooth Particle Hydrodynamics (SPH) [2]. This method was later generalized to fluid mechanic problems. One of the latest particle based methods is Moving Particle Semi-implicit (MPS) which was originally introduced by Koshizuka and Oka [3].

MPS method is applied for modeling a number of hydraulic phenomena such as dam break (Koshizuka et al.), breaking waves (Koshizuka et al.; Gotoh and Sakai and Gotoh et al.), jet breakup (Shibata et al.) and flow over spillways (Shakibaeinia and Jin) [4, 5]. Moreover, Gotoh et al. and Gotoh and Sakai developed a multi- phase MPS model for simulating gas- liquid and solid- liquid problems, sediment transport and floating bodies [1]. Ataie-Ashtiani and Farhadi compared different kernel functions and introduced a formulation for increasing the stability of the MPS model [6]. Zhang et al. proposed a new Laplacian model and used MPS method in simulating heat transfer problems [7]. Shibata and Koshizuka applied a 3D model to simulate behavior of rushing water into the ships and predicted the impact pressure on the deck [8]. Fayyaz added several variables such as surface tension to the multi- phase MPS model to improve its stability and accuracy [9]. Kondo et al. introducing an artificial pressure, suppressed pressure oscillation which is usually observed in MPS modeling [10].

Khayyer and Gotoh worked on conservation of momentum and introduced new formula for calculating pressure gradient and allowed a slight compressibility to suppress its fluctuations [5]. Later on, Khayyer and Gotoh proposed a higher order Laplacian formulation for stabilization and enhancement of pressure calculation [11]. Shakibaeinia and Jin replaced incompressibility in the original MPS model with a weakly incompressible model, by particle recycling strategy for boundary condition [12]. Tanaka and Masunaga tried to obtain a smooth pressure variation both in time and space and eliminate its oscillation [13]. Slamming problems such as liquid- liquid and solid- liquid collision were simulated by Lee et al. using MPS method [14]. To suppress the unphysical pressure oscillation, Kondo and Koshizuka proposed a new formulation for the source term of Poisson equation of pressure [15].

In practice, there are a large number of engineering problems belong to turbulent flow, and it is necessary to extend the original MPS method to the turbulent flow simulation. From the turbulent point of view, an incompressible SPH theory was combined with Large Eddy Simulation (LES) model by Gotoh et al, to investigate wave interaction with partially immersed breakwater [16]. Shao and Gotoh used a 2D Sub-Particle Scale (SPS) turbulence model based on

eddy viscosity assumption to simulate wave breaking on the beach by SPH method [17]. Two-equation k-ε turbulence model was chosen by Shao to couple with SPH scheme for simulating wave breaking on a slope [18]. To investigate the properties of the plunging waves, Shao and Ji combined numerical method of SPH with LES and used Smagorinsky model to simulate turbulence stresses [19]. Violeau and Issa reviewed turbulent models adapted to the SPH method from simplest model of mixing length to more sophisticated ones such as EARMS or LES [20].

In contrast with SPH, MPS method is usually used for modeling inviscid free surface flows and attempts to apply turbulence effects in these models has been very limited [21, 22, 23]. In the governing equations of Large Eddy Simulation, only Reynolds stress is a new term. So compared with the RANS, the governing equations of LES is easier to handle in MPS method. Gotoh et al. 2001 demonstrate advantage of simulation of free surface flow by LES simulation in MPS [24]. Fayyaz and Kolahdoozan tried to add the viscous effects of flow by means of constant eddy viscosity to their multi-phase MPS model [25]. Shirazpoor developed their multi-phase MPS method using Prandtl's mixing length theory and k-ε model in dam break problem [26, 27]. Pan et al. introduced an area-time average method to reduce the pressure fluctuation in MPS in their MPS-LES model and applied it to a 2D sloshing simulation [28]. Mosaffa and Tang et al. defined a refinement algorithm based on the particle splitting and increased the resolution of the whole simulation region in MPS multi-resolution model [29, 30]. Ikari et al. developed an erosion sub-model in their MPS model for analysis of large deformations of soil, due to wave induced erosion in sea cliffs. The model was further enhanced by utilizing sub-particle-scale suspended sediment load sub-model together with advection-diffusion equation by [31]. Harada et al. developed a DEM-MPS coupled method for reproduction of swash beach sediment transport processes in a gravel beach and investigated the formation/deformation processes of step series on the riverbeds in mountain [32, 33]. Gotoh and Khayyer provided an up-to-date comprehensive review on latest advancements related to particle methods with applications in coastal and ocean engineering [34]. They also highlighted future perspectives for further enhancement of applicability and reliability of particle methods for coastal and ocean engineering.

In this study, a particle-based numerical model is presented using MPS method to simulate different wave problems. The authors have developed their own code to simulate viscous fluid flow in the coastal waters. They have applied governing equations on fluid particles rather than mesh and solved them by MPS method to predict hydrodynamic parameters of solution domain. The effect of turbulence is calculated using three turbulence closures including constant eddy viscosity; Prandtl's mixing length and k-ε. Herein, results obtained for a number of wave problems from different turbulence closures combined with the developed MPS model are compared with experimental data or analytical solutions cited in the literature. It was found that considering turbulence effects improves the stability, accuracy and capability of the MPS model.

2. Governing Equations

Governing equations of viscous fluid flow include continuity and momentum equations can be represented as follows:

$$1/\rho \, D\rho/Dt + \nabla \mathbf{u} = 0 \quad (1)$$

$$D\mathbf{u}/Dt = -1/\rho \, \nabla p + \nu_t \nabla^2 \mathbf{u} + g \quad (2)$$

where $\boldsymbol{u}$= velocity vector, t= time, ρ= fluid density, P= pressure, ν_t= fluid eddy-viscosity and g= gravitational acceleration.

The pressure term in the momentum equations can be considered as an independent variable

which contains both the static and dynamic parts. Thus, by solving Poisson equation, the pressure term can be calculated for all particles. Poisson equation rewrites as follows [3]:

$$\nabla^2 P = {}^{\Delta\rho}/_{\Delta t^2} \tag{3}$$

In the MPS method, free surface is predicted automatically when all particles position were specified.

2.1. Model Discretization

In the MPS method the equations of continuity and momentum are converted to interaction equations of particles using different operators. All interactions between particles are limited to a specific distance known as efficient radius. The weighting of different neighboring particles within the efficient radius on the desired particle is calculated based on Kernel functions. In the present study following basic interaction model is used as the Kernel function [5]:

$$w(r) = \begin{cases} {}^{r_e}/_{r} - 1 & 0 < {}^{r}/_{r_e} \le 1 \\ 0 & 1 < {}^{r}/_{r_e} \end{cases} \tag{4}$$

where r= distance between two particles i and j, r_e= efficient radius and w= Kernel function.

This function is effective for saving computational time and memory and is efficient for avoiding clustering of particles and improves numerical stability [17].

The particle number density, actually a weighted average, can be defined in the following form by using the kernel function [3]:

$$\langle n \rangle_i = \sum_{j \neq i} w(|r_j - r_i|) \tag{5}$$

where n_i is the density of particle i in location r_i.

Since the fluid density is proportional to the particle number density [3], the continuity equation is satisfied if the particle number density is constant in incompressible fluids [6]. This constant value is denoted by n^0 and is called standard density. For n^0 we use particle number density in the initial state.

A gradient vector is evaluated between two neighboring particles. The gradient operator is modeled using the weight function and conserve linear and angular momentum. It can be expressed as [5]:

$$\langle \nabla \phi \rangle_i = {}^{d}/_{n^0} \sum_{j \neq i} \left[(\phi_i + \phi_j) - 2\hat{\phi}_i \Big/ |r_j - r_i|^2 (r_j - r_i) w(|r_j - r_i|) \right] \tag{6}$$

where ϕ= a physical quantity, d= number of dimension (for two dimensions is replaced with 2), r_i = location vector for particle i, and ϕ' = minimum amount of ϕ belonging to the neighboring particles in the efficient radius:

$$\phi_i' = \min(\phi_j) \quad \text{for} \quad \{w(|r_j - r_i|) \neq 0\} \tag{7}$$

The presented Laplacian model has a conservative form and can be written as [3]:

$$\langle \nabla^2 \phi \rangle_i = {}^{2d}/_{n^0 \lambda} \sum_{j \neq i} [(\phi_j - \phi_i) w(|r_j - r_i|)] \tag{8}$$

In the above equations, λ is a coefficient defined as:

$$\lambda = \int w(r) r^2 dv \Big/ \int w(r) dv \tag{9}$$

2.2. Turbulence Closures

Since the flow in this study is viscous and turbulent, Prandtl's mixing length theory and k-ε models are used in addition to constant eddy viscosity to consider shear stresses in the flow

domain.

According to Prandtl's mixing length model [35,36] which is widely used in estuaries and coastal waters [37] eddy viscosity ν_t can be written as:

$$\nu_{t,i} = \kappa u_{*i} z_i \left(1 - {}^{z_i}/_{H}\right) \quad (10)$$

where, $\nu_{t,i}$= turbulent eddy viscosity for particle i, κ= von Karman's constant, u_{*_i}= shear velocity for particle i, z_i= vertical distance of particle i from the bed and H= total water depth.

According to k-ε turbulent model [38] eddy viscosity ν_t can be written as:

$$\nu_{t,i} = C_\mu \, {}^{k_i^2}/_{\varepsilon_i} \quad (11)$$

where k_i= turbulence kinetic energy for particle i, ε_i= energy dissipation rate for particle i and C_μ is a constant= 0.09.

Lagrangian form of convection equation for turbulence kinetic energy, k can be written as [20, 38]:

$${}^{Dk}/_{Dt} = P_k - \varepsilon + \nabla\left[\left(\nu + {}^{\nu_t}/_{\sigma_k}\right)\nabla k\right] \quad (12)$$

where σ_k is a constant =1.0.

This equation is analogous to the convection-diffusion equation where the production rate of kinetic energy P_k is similar to the source term, while energy dissipation ε is similar to the sink term P. In the MPS method the convection equation for k reads as:

$${}^{\Delta k}/_{\Delta t} = P_{k_i} - \varepsilon_i + {}^{2d\nu_{k,i}}/_{n^0\lambda} \sum_{j\neq i}\left[\left(k_j - k_i\right) w\left(|r_j - r_i|\right)\right] \quad (13)$$

where:

$$\nu_{k,i} = \nu + {}^{\nu_{t,i}}/_{\sigma_k} \quad (14)$$

in vector form, the source term P is [20]:

$$P = \nu_t S^2 \quad (15)$$

However, for preventing any overestimation of k in cases with high rates of strain, the non-isotropic turbulence should be limited. Therefore, a linear strain variation rate is considered for high deformations and the source term of particle i is limited as follows [20]:

$$P_{k_i} = \min\left(\sqrt{C_\mu}, C_\mu S_i \, {}^{k_i}/_{\varepsilon_i}\right) k_i S_i \quad (16)$$

For calculating the scalar mean rate of strain S one can write [18]:

$$S = \left[2\left({}^{\partial u}/_{\partial x}\right)^2 + 2\left({}^{\partial v}/_{\partial y}\right)^2 + \left({}^{\partial u}/_{\partial y} + {}^{\partial v}/_{\partial x}\right)^2\right]^{1/2} \quad (17)$$

The energy dissipation rate ε can be written as [18, 38]:

$${}^{D\varepsilon}/_{Dt} = \nabla\left[\left(\nu + {}^{\nu_t}/_{\sigma_\varepsilon}\right)\nabla\varepsilon\right] + {}^{\varepsilon}/_{k}\left(C_{\varepsilon,1}P_k - C_{\varepsilon,2}\varepsilon\right) \quad (18)$$

where σ_ε, $C_{\varepsilon,1}$ and $C_{\varepsilon,2}$ are empirical constants= 1.3, 1.44 and 1.92 respectively.

The MPS form of Equation (18) is as follows:

$${}^{\Delta\varepsilon}/_{\Delta t} = {}^{2d\nu_{\varepsilon,i}}/_{n^0\lambda} \sum_{j\neq i}\left[\left(\varepsilon_j - \varepsilon_i\right) w\left(|r_j - r_i|\right)\right] + {}^{\varepsilon_i}/_{k_i}\left(C_{\varepsilon,1}P_{k_i} - C_{\varepsilon,2}\varepsilon_i\right) \quad (19)$$

where:

$$\nu_{\varepsilon,i} = \nu + {}^{\nu_{t,i}}/_{\sigma_\varepsilon} \quad (20)$$

In the current study, a two-dimensional vertical model was developed considering the turbulence effect of the flow in the formulation, though the proposed method can be extended to three dimensions.

3. Solution Procedure

The governing equations of flow were solved semi-implicitly. To speed up the convergence the Projection method was deployed in which discretization of Navier-Stokes equations were completed in two half time steps. In the first half time step (prediction step) governing equations were solved in the presence of viscosity and gravity terms without enforcing incompressibility, while the pressure were disregarded. In the second half time step (correction step), the results obtained in the previous time step were modified in the presence of pressure gradient. In other words, the pressure term was used to update the particles velocity calculated from the prediction step [15, 17]. In mathematical expression, the Navier-Stokes equations for the first half time step can be written as:

$$\mathrm{D}\mathbf{u}/_{\mathrm{Dt}} = \nu_t \nabla^2 \mathbf{u} + g \tag{21}$$

To solve this equation, primarily, eddy viscosity should be computed.

In Prandtl's mixing length model, the eddy viscosity was computed based on velocity and position of particles according to Equation (10).

In k-ε model, in each time step, the solution algorithm followed Equation (11) to (20).

After solving Equation (21) explicitly, velocity components variations ($\Delta\mathbf{u}$) of all particles were obtained. Then, modified velocity and positions were calculated for each particle as follows:

$$\mathbf{u}^{t+1/2} = \Delta\mathbf{u}^{t+1/2} + \mathbf{u}^{t} \tag{22}$$

$$r^{t+1/2} = \mathbf{u}^{t+1/2}\Delta t + r^{t} \tag{23}$$

where $\boldsymbol{u}^t$, r^t, $\boldsymbol{u}^{t+1/2}$, $r^{t+1/2}$ = current and intermediate particle velocity and position, respectively.

In the prediction step, mass conservation is not satisfied. It means the particle number density $n_i^{t+1/2}$ that are calculated at the end of first half time step deviates from the constant n^0. Therefore, a second corrective process is required to adjust the particle number densities to initial constant values prior to the time step. In the second half time step, the intermediate particle velocity $\boldsymbol{u}^{t+1/2}$ is updated implicitly through solving the Poisson pressure Equation.

To calculate particles pressure, Poisson pressure Equation was then solved with the following discretized representation [11]:

$$\langle \nabla^2 P_i^{t+1} \rangle = \rho/_{\Delta t^2} \, n_i^{t+1/2} - n^0/_{n^0} \tag{24}$$

where Δt= calculation time step and t denoted the step of calculation.

Since explicit calculation of Poisson pressure equation leads to model instability, it is recommended to solve it in full implicit form as a linear equations system. One of solving methods for this linear system is Cholesky solution [39].

Finally, given the amount of particles velocity components and position at time t+1/2 and pressure value, the second time step of Projection method was enforced. In this stage, pressure was included in the momentum equations in the following form:

$$\rho\, \mathrm{D}\mathbf{u}/_{\mathrm{Dt}} = -\nabla p \tag{25}$$

This equation was solved implicitly and new velocity components and particle positions in the next time step were calculated as follows:

$$\mathbf{u}^{t+1} = \Delta\mathbf{u} + \mathbf{u}^{t+1/2} \tag{26}$$

$$r^{t+1} = \mathbf{u}^{t+1}\Delta t + r^{t+1/2} \tag{27}$$

The solution algorithm is illustrated in Figure 1.

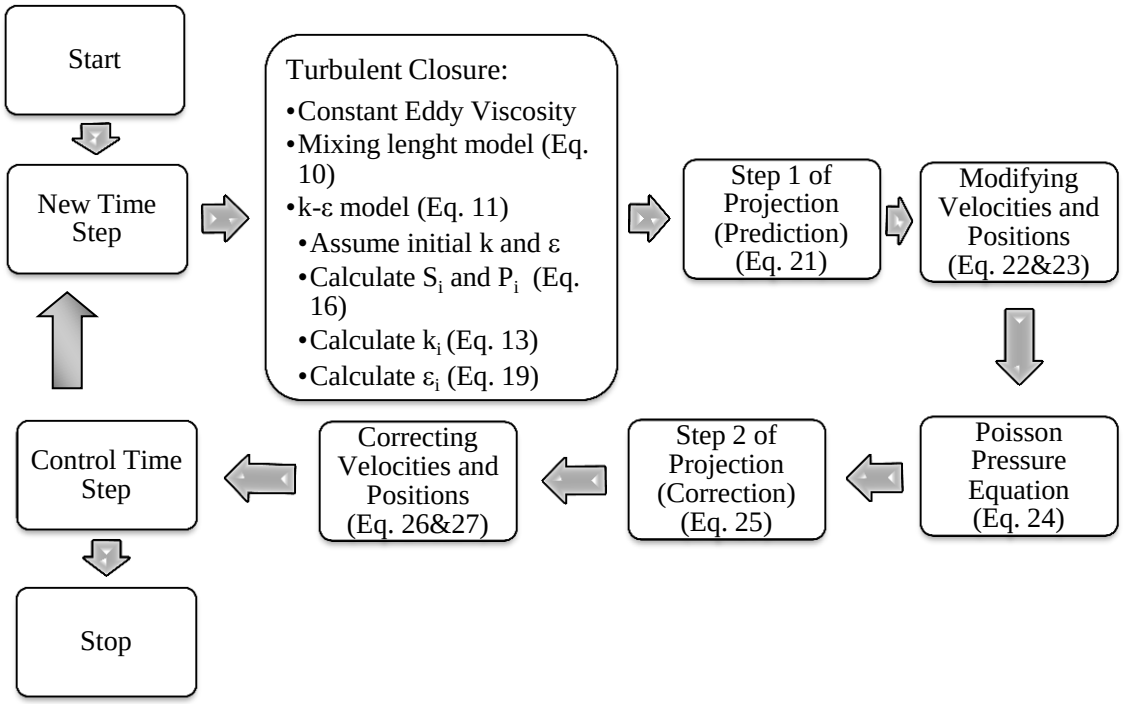


Figure 1. Solution algorithm of the present MPS model

4. Boundary Conditions

4.1. Free Surface

Free surface was defined as the location at which particles density is less than a certain value. Following condition is defined for free surface particle recognition [39]:

$$n_i < \beta n^0 \quad (28)$$

where β = threshold coefficient which is define 0.97 [1, 6, 9].

The standard or zero pressure value would be assigned in each time step to particles in this location and no additional computations were necessary.

4.2. Bed Boundary

Along solid boundary, particles position in the impermeable channel bed and walls were invariable and liquid particles were not able to penetrate into this solid layer. In all time steps, the governing equations were solved for near solid boundary particles to repulse the inner fluid particles accumulating in the vicinity of wall.

To model the no-slip condition in the vicinity of solid boundary, each particle near the boundary was checked for not to penetrate inside the solid boundary [9, 17].

5. Results and Discussion

5.1. Still Water reservoir

A 0.2 m-long reservoir containing still water with 0.2 m depth was modeled by 2601

particles. Time step is equal to 0.003 s.

In Figure 2 pressure history for a point in the middle of reservoir on the bed is represented. The Standard MPS method suffers from some spurious pressure fluctuation. A comparison between pressures calculated by present model using up-to-date formulation for the pressure gradient [5, 11] and standard MPS models shows improvements in pressure calculation and reduction of pressure fluctuations, particularly near the solid boundaries.

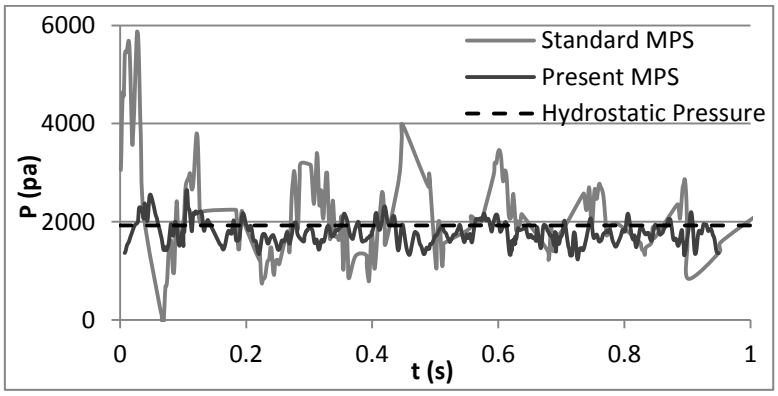


Figure 2. Computed pressure history on the bed (x= 0.1 m)

To represent the stability of computed pressure values, the pressure field in the middle of reservoir obtained from developed MPS model using no turbulence closures, is compared with hydrostatic values in Figure 3. It can be seen that pressure values are predicted near to hydrostatic line. It can be concluded that the numerical model is stable and predict pressure domain without fluctuation.

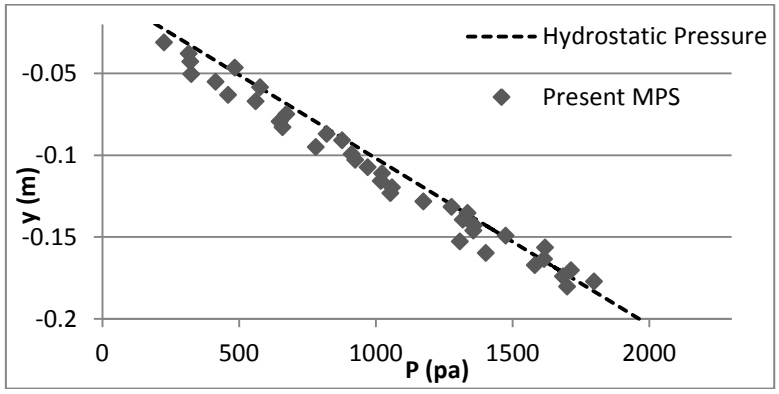


Figure 3. Comparison of computed pressure by present MPS model with hydrostatic values (x=0.1 m, t=0.2 s)

5.2. Solitary wave motion in a tank

Despite predominance of applying advanced pressure gradient formulation within static of fluid has been proven in the previous example; to evaluate the performance of the these new operators in the field of waves dynamic and their effects on the improvement of numerical calculations, they are applied in another test case.

In this test, wave motion in a tank with vertical walls was studied. The Wave tank was 3 m long with 0.5 m water depth. Solitary waves with different heights of 0.15 to 0.3 m were

generated at the left side of the tank and were propagated to the right. After collision of waves to the upright wall, run-up occurred.

Waves were generated similar to Monaghan and Kos experiments with the following equation [40]:

$$\eta = {H}\Big/{\mathrm{Cosh}^2\left(x\sqrt{\frac{3H}{4h^3}}\right)} \quad (29)$$

where η = free surface elevation, H= wave height, h= water depth and x= distance parallel to wave motion.

The wave profile equation was considered as the initial condition. According to solitary wave theory the vertical velocity is zero. The horizontal velocity profile U was introduced as follows [40]:

$$U = {\eta}/{h}\sqrt{gh} \quad (30)$$

In order to select basic variables such as time step and particle distance, the Courant number criterion was applied which can be written as:

$$Cr = {\Delta t\, V_{max}}/{r_0} \quad (31)$$

where r_0= initial distance between particles, Δt= time step, V_{max}= maximum flow velocity and $0 < Cr \leq 1$ is the Courant number. Shakibaeinia and Jin used $Cr = 0.25$, Ataie-Ashtiani and Farhadi employed $Cr = 0.2$, while Fayyaz and Kolahdoozan and Shobeyri and Afshar set $Cr = 0.1$ to have a stable solution [6, 12, 25, 41]. Factor 0.1 ensures that the particle moves only a fraction of the particle spacing in a time step.

Using Courant number maximum acceptable time step is gained according to particle size. To keep calculation stability an appropriate time step should be chosen. In this test case, particle diameter is equal to 0.035 m; the flow domain was modeled with 1600 particles in average and time step of 0.003 s, which satisfy considered Courant number.

In this test, turbulent models were not included in the model and the fluid was considered non-viscous. In Figure 4 non-dimensional values of run-up calculated by the MPS model were compared with experimental data of Camfield and Street, the results of MAC model of Chan and Street and SPH model of Monaghan and Kos [40].

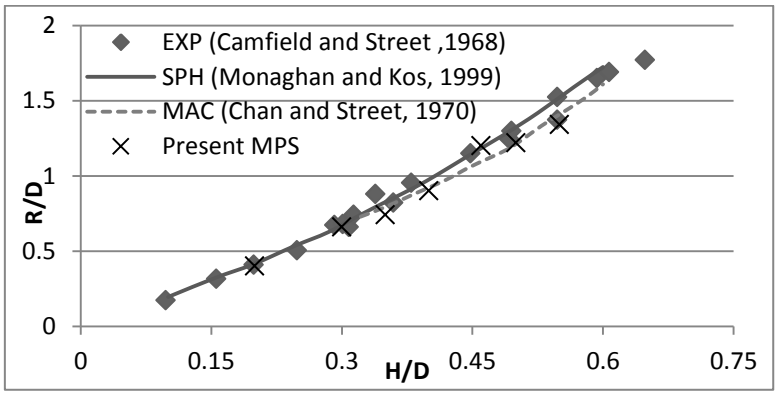


Figure 4. Comparison of present MPS model results with experimental data, MAC model and SPH model

Maximum computational errors were 4.5% and 4.1% for SPH and the present MPS methods respectively. In addition, MAC model has 4.3% error in comparison with laboratory results. It can be seen that the results of the developed model are closer to the experimental data in

comparison with the previous models.

From Figure 4 according to the present MPS model results, the following relationship is suggested to express the variation of wave run-up with water depth and wave height:

$$R/h = 2.862(H/h)^{1.230} \quad (32)$$

where *R*= wave run-up.

Water surface level and pressure predicted by the developed model for H/h equals to 0.4 are shown in Figure 5. Pressure field is presented in three time steps: A) before wave collision to the right wall, when a high pressure zone is formed at the end of the channel due to wave impact effect, B) highest run-up time when pressure field is decreased due to steady condition at maximum run-up and C) after collision when backwash happens and wave moves in the channel in a reverse direction.

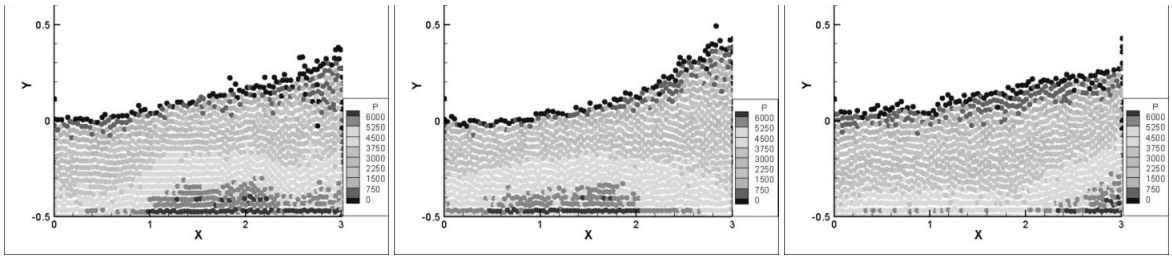


Figure 5. Computed water surface and pressure field (H/h=0.4)

Moreover, predicted velocity domain in two time step, before and after run-up, are displayed in Figure 6.

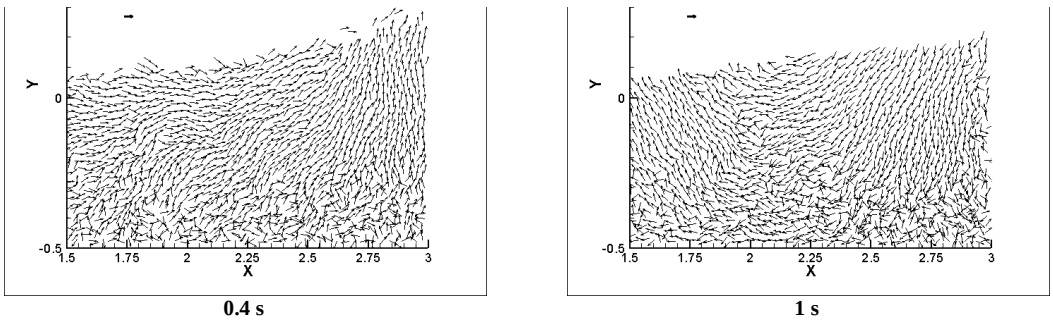


Figure 6. Computed velocity field (H/h=0.4)

It should be noted that except near the bed, velocity vectors are parallel to each other that shows rising wave front to the vertical wall before run-up and descending wave forehead after run-up.

5.3. Tsunami run-up on a slope

In this test the tsunami motion toward a slope was investigated. Initial wave profile was generated by Equation (29). Vertical velocity was assumed equals to zero and horizontal velocity was calculated from Equation (30).

In this case a 3 m long channel was considered. The slope angle of the beach was assumed 45^{o} and a wave height of 0.2 m was considered for modeling purposes. Water depth 'h' varied in

the range of 0.5 to 1 m. Wave was generated at the left side of the channel, propagated to the right and ran-up on the inclined beach (Figure 7).

Particle diameter is equal to 0.033 m; the flow domain was modeled with 2500 particles in average and time step of 0.003 s.

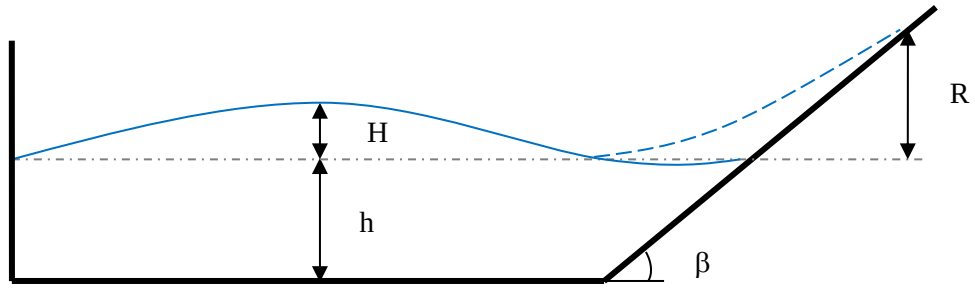


Figure 7. Tsunami run-up on a slope

Wave run-up on a slope can be estimated from empirical equations given in the literature. One of the recent relationships for long wave run-up on an impermeable smooth slope is presented by Muller, which considers wavelength as [42]:

$$R/h = 1.25\left(\pi/2\beta\right)^{0.2}\left(H/h\right)^{1.25}\left(H/L\right)^{-0.15} \quad (33)$$

where *L*= wavelength.

In theory solitary wave is infinitely long and it is not worth from engineering viewpoint. For practical purposes, its wavelength can be defined where 95% of area under wave profile is contained within this distance [43]:

$$L = 2.12h\sqrt{h/H} \quad (34)$$

In Figure 8 the calculated run-up by the developed model are compared with Equation (33). It can be seen that results of the k-ε model are closer to the results of the empirical equation.

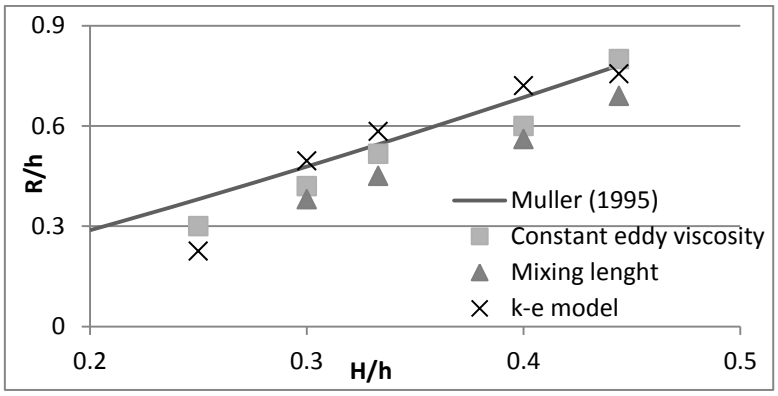


Figure 8. Comparison of present MPS model results with empirical relationships

Furthermore, run-up error analysis is carried out for various turbulence models. In constant eddy viscosity error is 5.5%, while in mixing length and k-ε model this value is 10% and 3%, respectively. This shows the superiority of the k-ε model.

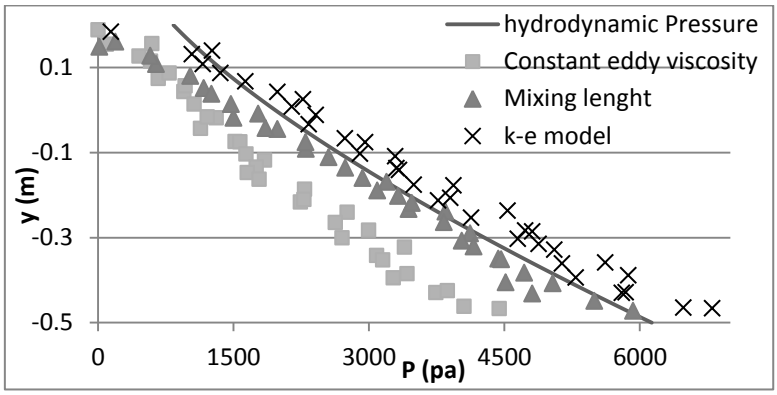


Figure 9. Comparison of computed pressure (H/h=0.4, x=3 m, t=0.5 s) by different turbulence closures with analytical pressure

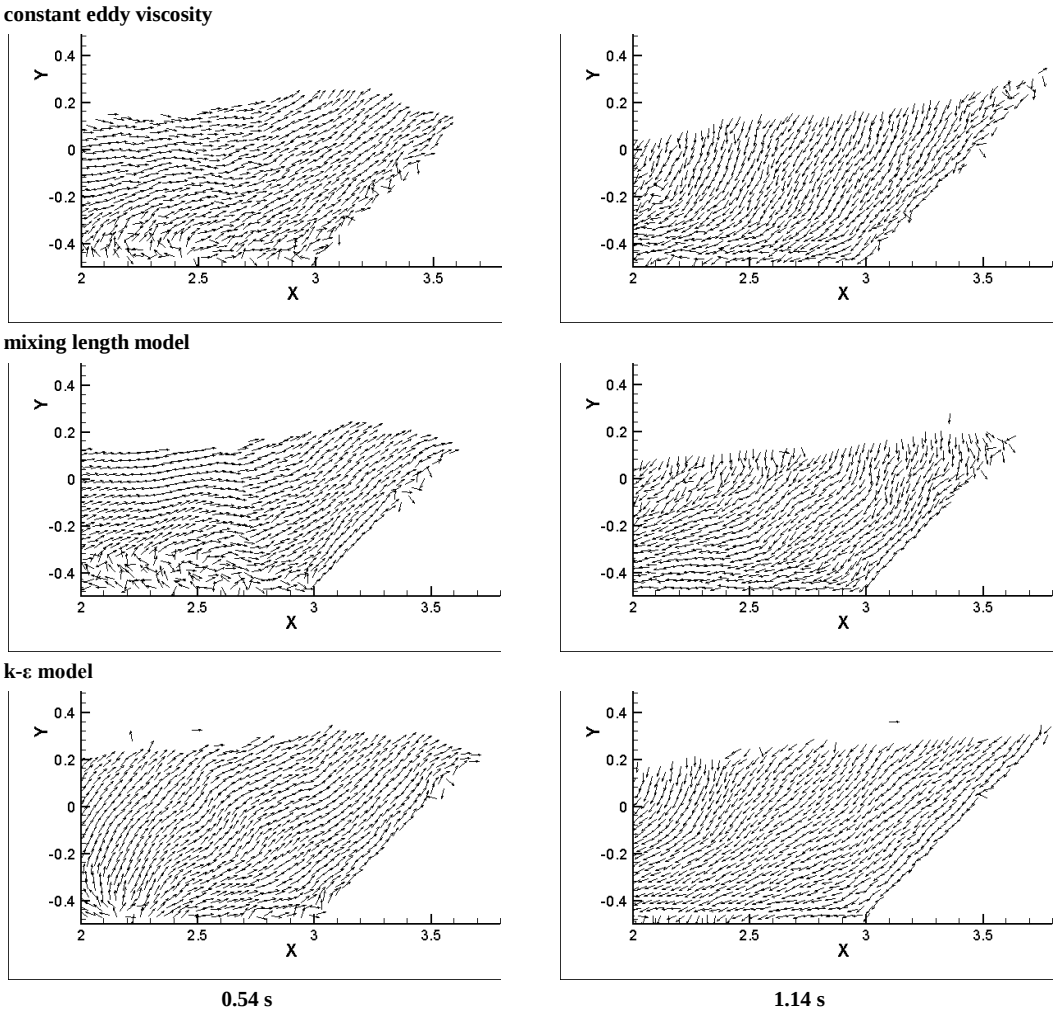


Figure 10. Computed velocity field (H/h=0.4)

In Figure 9, computed pressure field in the toe of the slope on the channel invert at time 0.5 s (before complete wave run-up on the slope) is compared with analytical values of water waves as [43]:

$$P = \rho g(\eta K_p - z) \quad (35)$$

where $P =$ pressure and $K_p =$ dynamic pressure coefficient.

From Figure 9 it can be concluded that constant eddy viscosity model underestimated pressure values in average by 45%, while mixing length model estimated it by 21%. k-ε model prediction has 4% mean-error which shows a better agreement with the analytical results. Computed velocity field using various turbulent models before and after run-up, are demonstrated in Figure 10.

Parallel velocity vectors show the progressive wave fronts toward the inclined wall before run-up. After run up however velocity vectors show properly the returning wave. Among turbulent models, k-ε velocity predictions are smoother and without fluctuations. This is more evident in the vicinity of the solid boundaries of bed and wall.

5.4. Landslide-generated water wave

To simulate landslide-generated waves, a rigid wedge, triangular in cross section (0.5×0.5 m) sliding into water along an inclined plane of 45° was considered [44,45]. Water depth was assumed 0.4 m and the bottom of the wedge was initially just above the initial free water surface (Figure 11).

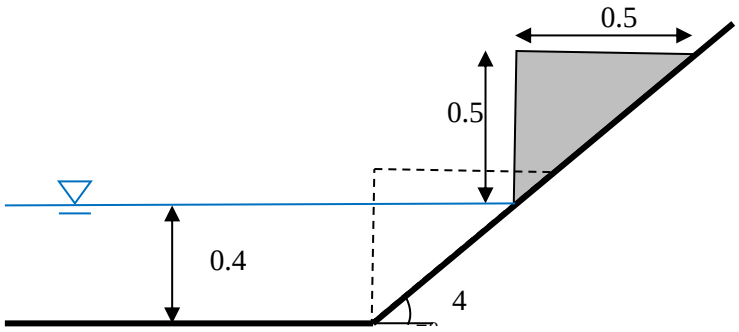


Figure 11. Rigid wedge sliding on the slope into water

Motion of the wedge in time was determined based on the following equation:

$$\text{vertical displacement} = 0.87 * t^2 + 0.2321 * t - 0.0048 \quad (36)$$

To model this case a channel with 0.4 m height and 6 m length was considered. The total numbers of 2444 particles was considered in the computational domain. Time step was selected equal to 0.003 second and initial wave profile was produced by Equation (29). Vertical velocity was assumed equals to zero and horizontal velocity was calculated from Equation (30).

Generated wave and water level variation at various times and for different turbulence models are compared with experimental measurements of Heinrich in Figure 12. From this comparison it can be seen that predicted water surface elevations by k-ε turbulence model are more accurate.

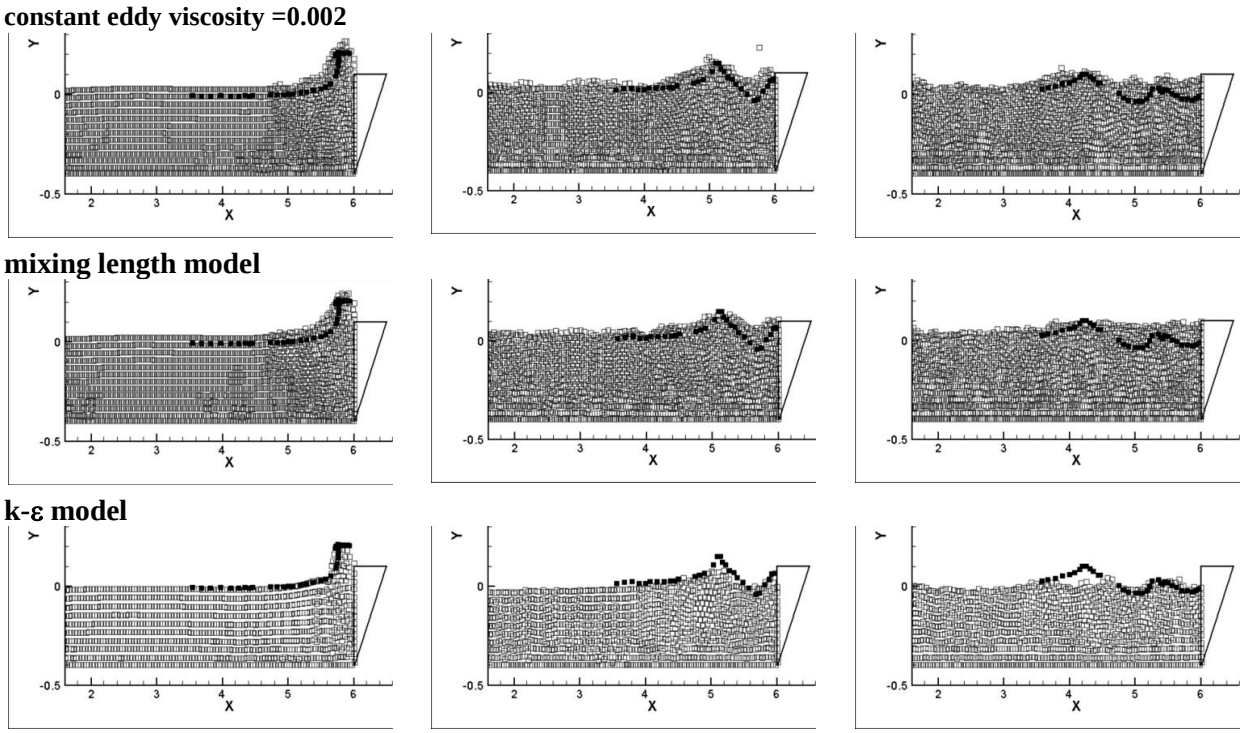


Figure 12. Comparison of computed water surface with experimental data (black dots)

Errors in water surface calculation for various turbulent models are presented in Table 1. It can be seen that k-ε model accuracy was considerably more than the other two models.

Table 1. Water surface error analysis for different modeling alternative

Time (s)	constant eddy viscosity	mixing length	k-ε
0.6	4%	4.3%	1.6%
1	5%	4.9%	3.5%
1.5	6.8%	6.7%	4.3%

Figure 13 shows the pressure and velocity field in the water body after 1 second using k-ε model. As can be seen in Figure 13, velocity vectors behind the wave front are downward while the velocity vectors in front of its forehead are upward showing the advancing wave to the end of the channel. .In addition, a relatively high pressure zone due to impact is observed prior to wave crest, due to wave progress.

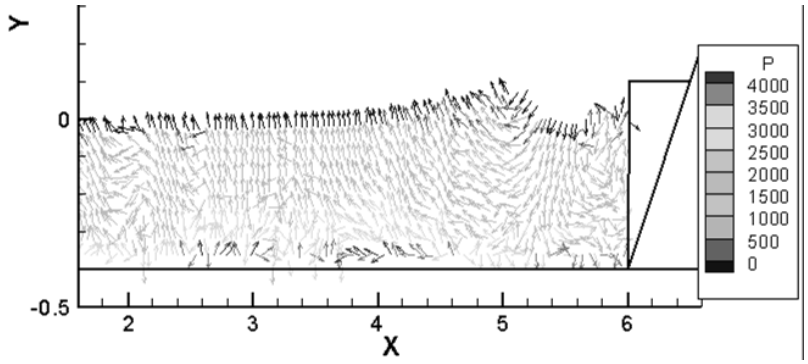


Figure 13. Computed velocity and pressure field after 1 s using k-ε model

6. Conclusion

In this article, a novel particle-based numerical model is developed using Moving Particle Semi-implicit (MPS) to simulate nonlinear hydrodynamic behavior of free surface water waves. In contrast with previous MPS models, with the aim of simulating turbulent nature of wave flows, the developed model has equipped with three turbulence models including constant eddy viscosity, Prandtl's mixing length theory and k-ε model. In addition, higher order of MPS operators was applied to suppress numerical oscillation in comparison with previous studies. The effect of applying various turbulence models on the MPS method in wave evolution is studied. To investigate the accuracy of the developed model, some wave problems such as wave propagation, wave run-up and landslide generated waves are solved numerically. Comparison of obtained results and data cited in the literature shows the ability of developed model in simulating water surface and pressure distribution in such complicated situation of wave motion. The stability and accuracy of MPS in modeling wave problems can be increased by implementing more complicated turbulence models such as k-ε instead of common constant eddy viscosity. This can be seen clearly in tsunami run-up and landslide simulations. Moreover, pressure field which is calculated implicitly and is predicted more precisely. Therefore, the model is capable to simulate complex and turbulent flows such as wave impacts, as it shown in tsunami test-case. In other word, in complicated intensive hydraulic gradient problems such as near shore, or in real case studies in which the effect of viscosity should be considered, the MPS model applying advanced turbulent models such as k-ε is more accurate than previous numerical models.

7. References

1. Gotoh, H., Sakai, T. (2006), Key issues in the particle method for computation of wave breaking, Coast. Eng., 53, 171-179.
2. Monaghan, J.J. (1994), Simulating free surface floes with SPH, J. Comput. Phys. 110, 399-406.
3. Koshizuka, S., Nobe, A., Oka, Y. (1998), Numerical analysis of breaking waves using the moving particle semi-implicit method, Int. J. Numeri. Meth. Fl., 26, 751-769.
4. Shakibaeinia, A., Jin Y.C. (2009), Lagrangian modeling of flow over spillways using the moving particle semi- implicit methods, Proceeding of 33rd IAHR Congress, Vancouver, Canada, 1809-1816.
5. Khayyer A., Gotoh, H. (2009), Modified moving particle semi-implicit methods for the prediction of 2D wave impact pressure, Coast. Eng., 56, 419-440.

6. Ataei-Ashtiani, B., Farhadi, L. (2006), A stable moving –particle semi-implicit method for free surface flows, Fluid Dyn. Res., 38, 241-256.
7. Zhang, S., Morita, K. Fukuda, K. and Shirakawa, N. (2006, An improved MPS method for numerical simulations of convective heat transfer problems, Int. J. Numeri. Meth. Fl., 51, 31-47.
8. Shibata, K., Koshizuka, S. (2007), Numerical analysis of shipping water impact on a deck using a particle method. Ocean Eng., 34,585-593.
9. Fayyaz, M. (2008), Numerical modeling of interaction between waves and coastal structures, M.S. thesis, Department of Civil and Environmental Engineering, Amirkabir University, Tehran, Iran.
10. Kondo, M., Suto, K., Sakai, M. and Koshizuka, S. (2008), Incompressible free surface flow analysis using moving particle semi-implicit method, Joint International Workshop: Nuclear Technology and Society- Needs for Next Generation, Berkeley, California, USA.
11. Khayyer A., Gotoh, H. (2010), A higher order Laplacian model for enhancement and stabilization of pressure calculation by the MPS method, App. Ocean Res., 32, 124-131.
12. Shakibaeinia, A., Jin Y.C. (2010), A weakly compressible MPS method for modeling of open-boundary free-surface flow, Int. J. Numeri. Meth. Fl., 63, 1208-1232.
13. Tanaka, M., Masunaga, T. (2010), Stabilization and smoothing of pressure in MPS method by quasi-compressibility, J. Comput. Phys., 229, 4279-4290.
14. Lee, B.H., Park, J.C., Kim, M.H., Jung, S.J., Ryu, M.C. and Kim, Y.S. (2010), Numerical simulation of impact loads using a particle method, Ocean Eng., 37, 164-173.
15. Kondo, M., Koshizuka, S. (2011), Improvement of stability in moving particle semi-implicit method, Int. J. Numeri. Meth. Fl., 65(6), 638-654.
16. Gotoh, H., Shao, S.D. and Memita, T. (2004), SPH-LES model for numerical investigation of wave interaction with partially immersed breakwater, Coast. Eng. J., 46(1), 39-63.
17. Shao, S.D., Gotoh, H. (2005), Turbulence particle models for tracking free surfaces, J. Hydraul. Res., 43(3), 276-289.
18. Shao, S.D. (2006), Simulation of breaking wave by SPH method coupled with k-ε model, J. Hydraul. Res., 44(3), 338-349.
19. Shao, S.D., Ji, C. (2006), SPH computation of plunging waves using a 2D sub-particle scale (SPS) turbulence model, Int. J. Numeri. Meth. Fluid, 51, 913-936.
20. Violeau, D., Issa, R. (2007), Numerical modeling of complex turbulent free-surface flows whit the SPH method: and overview, Int. J. Numeri. Meth. Fl., 53, 277-304.
21. Koshizuka, S., Oka, Y. (1996), Moving particle semi-implicit method for fragmentation of incompressible fluid, Nucl. Sci. Eng., 123(3), 421-34.
22. Suzuki, Y., Koshizuka, S. and Oka, Y. (2007), Hamiltonian moving-particle semi-implicit (HMPS) method for incompressible fluid flows, Comput. Meth. Appl. Mech. Eng., 196, 2876-2894.
23. Ataei-Ashtiani, B., Shobeyri, G. and Farhadi, L. (2008), Modified incompressible SPH method for simulating free surface problems, Fluid Dyn. Res., 40, 637-661.
24. Gotoh, H., Shibahara, T. and Sakai, T. (2001), Sub-particle-scale turbulence model for the MPS method- Lagrangian flow model for hydraulic engineering, Comput. Fluid Dyn. J., 9(4), 339-347.
25. Fayyaz, M., Kolahdoozan, M. (2010), Development of 3D MP-MPS model for flow pattern prediction during the intensive hydraulic gradient, J. Hydraul., 4(4), 33-50.
26. Shirazpoor, S. (2010), Numerical modeling of fluid flows in the vicinity of floating breakwater, M.S. thesis, Department of Civil and Environmental Engineering, Amirkabir

University, Tehran, Iran.
27. Kolahdoozan, M., Ahadi, M., Shirazpoor, S. (2014), Effect of turbulence closure models on the accuracy of moving particle semi-implicit method for the viscous free surface flow, Scientia Iranica Transaction A-civil Engineering, 21(4), 1217-1230.
28. Pan, X., Zhang, H. and Sun, X. (2012), Numerical simulation of sloshing with large deforming free surface by MPS-LES method, China Ocean Eng., 26(4), 653-668.
29. Mosaffa, M. (2014), Variable Resolution in WC-MPS Method for Fluid Flow Problems, MS thesis, University of Regina, Canada.
30. Tang, Z., et al. (2016), Numerical simulation of 3D violent free-surface flows by multi-resolution MPS method, J. Ocean Eng. Mar. Energy, 2, 355–364.
31. Ikari, H., et al. (2015), MPS-based Simulation of Scouring Due to Submerged Vertical Jet with Sub-Particle-Scale Suspended Sediment Model, J. of Japan Society of Civil Eng., Ser. B2 (Coastal Eng.) 71, 19-24.
32. Harada, E., et al. (2017), Numerical simulation for sediment transport using MPS-DEM coupling model, Advances in Water Resources, in press.
33. Harada, E., et al. (2018), Numerical Investigation of the Morphological, Dynamics of a Step and Pool Riverbed Using DEM-MPS.", Journal of Hydraulic Engineering, 144(1)
34. Gotoh, H., Khayyer, A. (2018), On the state-of-the-art of particle methods for coastal and ocean engineering, Coastal Eng. J., in press.
35. Schlichting, H. (1960), Boundary layer theory, McGraw-Hill Book Company, USA, 647.
36. Henderson, F.M. (1966), Open channel flow, Macmillan Publishing Co., Inc. New York, USA.
37. Kolahdoozan, M. (1999), Numerical modelling of geomorphological processes in estuarine waters, Ph.D. thesis, Department of Civil and Environmental Engineering, University of Bradford, Bradford, U.K.
38. Rodi, W. (1980), Turbulent models and their application in hydraulics- a state of the art review, Book Publication of IAHR, Delft, Netherlands.
39. Datta, B.N. (1995), Numerical linear algebra and applications, Brooks/Cole Publishing Company, USA.
40. Monaghan, J.J., Kos, A. (1999), Solitary waves on a cretan beach, J. of Waterw. Port Coast. Ocean Eng., 125(3), 145-154.
41. Shobeyri, G., Afshar, M.H. (2010), Simulating free surface problems using Discrete Least Squares Meshless method, Computers & Fluids, 39, 461–470.
42. Gedik, N., Irtem, E. and Kabdasli, S. (2005), Laboratory investigation on tsunami run-up, Ocean Eng., 32, 513-528.
43. Dean, R.G., Dalrymple, R.A. (1991), Water wave mechanics for engineers and scientists, Advanced Series on Ocean Engineering, World Scientific, Singapore.
44. Qiu, L.C. (2008), Two-dimensional SPH simulation of landslide-generated water wave, J. Hydraul. Eng., 134(5), 668-671.
45. Heinrich, P. (1992), Nonlinear water waves generated by submarine and aerial landslide, J. Waterw. Port Coast. Ocean Eng., 118(3), 249-266.